Effect of high-dose cyclophosphamide on ultrastructural changes and gene expression profiles in cardiomyocytes of C57BL/6J mice

Takuro Nishikawa (adu44150@ams.odn.ne.jp)
Kagoshima University Graduate School of Medical and Dental Sciences
Emiko Miyahara
Kagoshima University Graduate School of Medical and Dental Sciences
Ieharu Yamazaki
BML Inc. Research Institute
Hiroko Hagiwara
Cell Innovator Inc, Venture Business Laboratory of Kyushu University
Kazuro Ikawa
Hiroshima University
Shunsuke Nakagawa
Kagoshima University Graduate School of Medical and Dental Sciences
Yuichi Kodama
Kagoshima University
Yoshifumi Kawano
Kagoshima University Graduate School of Medical and Dental Sciences
Yasuhiro Okamoto
Kagoshima University Graduate School of Medical and Dental Sciences

Article

Keywords:

Posted Date: May 18th, 2022

DOI: https://doi.org/10.21203/rs.3.rs-1629925/v1

Abstract

The pathogenesis of cyclophosphamide (CY)-induced cardiotoxicity remains unknown, and methods for its prevention have not been established. To elucidate acute structural changes in myocardial cells and pathways leading to myocardial damage in mice treated with high-dose CY, we performed detailed pathological analyses of myocardial tissue obtained from C57BL/6J mice that received high-dose CY. In addition, we analyzed the genome-wide cardiomyocyte expression profile of mice that received high-dose CY. Treatment with CY caused marked ultrastructural aberrations with electron microscopy, although these could not be observed with optical microscopy. Expansion of the transverse tubule and sarcoplasmic reticulum, turbulence of myocardial fiber travel, and low contractile protein density in cardiomyocytes were observed. High-dose CY treatment changed cardiomyocyte expression of 1,210 genes associated with cell-cell junctions, inflammatory responses, cardiomyopathy, and cardiac muscle function, as detected by microarray analysis ($|$Z-score$|$ > 2.0). The expression of functionally important genes related to myocardial contraction and the regulation of calcium ions was validated using real-time polymerase chain reaction analysis. Our results of gene expression profiles, functional annotation clustering, and the Kyoto Encyclopedia of Genes and Genomes pathway functional classification analysis suggest that cardiotoxicity induced by CY is associated with a disruption of the Ca^{2+} signaling pathway.

Introduction

Cyclophosphamide (CY) is an old alkylating agent and is one of the most frequently used antitumor drugs[1, 2]. Although there are a variety of conditioning agents available for hematopoietic stem cell transplantation (HSCT) to treat hematological malignancies, bone marrow failure, or immunodeficiency, most standard treatment regimens and most commonly performed conditioning modalities include high-dose CY[2]. In recent years, post-transplant high-dose CY therapy has also become popular worldwide as a potent graft-versus-host disease prophylaxis, especially in human leukocyte antigen haploidentical HSCT settings[3, 4]. Therefore, the use of high-dose CY therapy is increasing.

Cardiotoxicity is the dose-limiting toxicity of CY. It is well documented that acute cardiac failure occurs within a week in a few patients receiving high doses of CY, with unpredictable and fatal consequences[4–6]. However, the detailed mechanism of cardiotoxicity of CY is unclear and no preventive measures have been established. As outcomes of HSCT have improved, these potentially fatal complications have been explored further.

Cyclophosphamide, a prodrug, is converted to the cytotoxic metabolites 4-hydroxycyclophosphamide (HCY) and aldocyclophosphamide (AldoCY) by the cytochrome P-450 (CYP) enzyme system (CYP2B6, 2C9, 2C19 and 3A4) in the liver. Both metabolites then circulate in the body and passively enter other cells. AldoCY undergoes an intracellular β-elimination reaction to form phosphoramide mustard (PM), which exhibits alkylating activity. Acrolein is formed as a byproduct of this process. On the other hand, if

intracellular aldehyde dehydrogenase 1 activity is high, AldoCY is detoxified to o-carboxyethyl-phosphoramide mustard (CEPM), an inactive metabolite [7, 8] (Fig. 1).

Previously, we evaluated myocardial cell injury associated with CY by exposing the rat cardiac myocardial cell line H9c2 to CY metabolites,[9, 10] which, we hypothesized, would increase myocardial cell injury due to the increases in acrolein and apoptosis. Co-exposure to the antioxidant and acrolein scavenger N-acetylcysteine (NAC) [11] suppresses myocardial cell injury induced by the CY metabolites. Our results suggest that this protective activity of NAC is due to apoptosis inhibition, decreased acrolein production, and increased CEPM production[9]. Since our report, other investigators have reported that acrolein may mediate CY-induced myocardial damage[12–15].

To study the acute myocardial cell structural changes and pathways of myocardial damage caused by cytotoxic CY metabolites, including acrolein in vivo, we planned to conduct a study using electron microscopy and comprehensive gene expression evaluation. Myocardial damage associated with CY administration in vivo has not been previously evaluated by microarray analyses (elucidating changes in gene-expression profile). Here, we examined gene expression profiles in mice exposed to CY to elucidate the mechanism of high-dose CY toxicity. Since acrolein is expected to be quickly absorbed by proteins and to not reach the myocardium when administered externally, this study was conducted primarily by administering CY[16–17].

Results

High-dose CY pharmacokinetics in mice

CY and metabolite levels were measured in plasma samples obtained from C57BL/6J mice that received 400–700 mg/kg of CY. Supplemental Fig. 1 shows concentration-time profiles for CY, HCY, and CEPM, and mice survival estimates. At 1 hour after the administration of CY (400 mg/kg), blood Cy levels were 25.3 μg/mL, while that at 4 hours after administration were < 1.50 μg/mL (below the limit of measurement); the corresponding levels of HCY and CEPM were 7.4 μg/mL and 0.6 μg/mL, and 26.5 μg/mL and 4.0 μg/mL, respectively. The AUC values for CY, HCY, and CEPM were 246.4 μM□h, 73.3 μM□h, and 269.1 μM□h, respectively. Meanwhile, at 1 and 3 hours after the administration of 500 mg/kg of CY, plasma levels of CY, HCY, and CEPM were 118.6 and 2.3, 92.4 and 3.0, and 69.1 and 16.9 μg/mL, respectively. The mean AUC values for CY, HCY, and CEPM were 1555.3 μM□h, 1092.5 μM□h, and 679.8 μM□h, respectively. Furthermore, for a dose of 700 mg/kg, CY, HCY, and CEPM levels were 251.2 ± 94.1 μM□h and 5.2 ± 6.4 μM□h, 57.7 ± 10.6 and 5.9 ± 4.4 μM□h, and 67.2 ± 40.0 μM□h and 26.4 ± 17.4 μM□h, respectively. The mean AUC values for CY, HCY, and CEPM were 4809.2 ± 1782.0 μM□h, 555.3 ± 115.1 μM□h, and 1305.4 ± 254.9 μM□h, respectively. When C57BL/6J mice were administered 400, 500, or 700 mg/kg of CY intraperitoneally, HCY and CEPM were produced in a manner comparable to that observed in humans (Supplemental Fig. 2). Various doses of CY were administered to the mice, and the maximum

dose of CY allowing mice to survive for more than a week was determined as 400 mg/kg/day for 2 days, which was a part of the administration schedule in this study (Supplemental Fig. 1).

Histopathological examination

Hematoxylin and eosin (HE) staining showed no difference between the CY-treated and NS-treated groups (Fig. 2A-D). However, electron micrograph analysis revealed ultrastructural alterations in cardiac tissue induced by CY administration. Treatment with CY (400 mg/kg × 2 days) caused marked ultrastructural aberrations (Fig. 2E-J). The nuclear membrane cavity showed generalized dissociation and localized heavily dilation (Fig. 2E). Lamellar bodies appeared in the cytoplasm, and expansion of the transverse tubule and sarcoplasmic reticulum were observed (Fig. 2E, F). Mitochondrial damage was observed, including expansion in size, cristae disintegration, and matrix loss (Fig. 2F). Fat droplets and vacuolar degeneration were also observed (Fig. 2F). In addition, lamellar bodies were found in the damaged mitochondria (Fig. 2F). The turbulence of myocardial fiber travel was observed (Fig. 2G, H). Furthermore, in the same myocardial cell, muscle contractile fiber structures were observed with contractile states different from those observed in other parts (Fig. 2I). Low-density contractile proteins in a cardiomyocyte were observed (Fig. 2J).

Identification of gene expression profiles associated with high-dose CY

We examined changes in expression of 52,141 genes using whole gene microarray analysis. Data have been made available in the National Center for Biotechnology Information Gene Expression Omnibus[18] and are accessible through the Gene Expression Omnibus Series (Accession Number GSE194073). At 7 days after CY administration, expression was up-regulated significantly in 675 genes, while significant down-regulation was observed in 535 compared to control values. Table 1 shows the 20 most up-regulated and 20 most down-regulated genes identified after CY exposure. At 7 days after acrolein administration, 280 genes showed significant up-regulation of expression and 299 genes showed significant down-regulation of expression. Between-group differences in gene expression were examined by scatterplot and clustering analyses (Figs. 3A and B). The number of expression-altered genes in the CY-treated mice was higher than that in the acrolein-treated mice (Fig. 3A). Figure 3B presents the genes involved in myocardial contraction in mouse cardiac tissue expressed at 3 hours after the administration of CY. Figure 3C shows gene expression patterns observed in samples treated with CY, including heat maps for genes whose expression differed between the CY and NS groups. Furthermore, the pattern of the heat map observed after CY administration was partially altered by NAC treatment. The pattern of the heat map of acrolein administration was similar to that of NS.

Gene-enrichment and Functional annotation analysis

Initial data were generated based on the results of NS and CY administration groups and were categorized based on several annotation categories, including protein-protein interactions and Gene

Ontology (GO) terms (p-values of < 0.05). The five most frequent functional annotation clustering categories obtained from samples treated with CY for 3 hours are shown in Table 2. As associated with myocardial dysfunction, genes related to dilated cardiomyopathy, arrhythmogenic right ventricular cardiomyopathy, and hypertrophic cardiomyopathy were significantly altered by CY administration. The generation of functionally regulated gene groups was dependent on reference to the Kyoto Encyclopedia of Genes and Genomes (KEGG) pathway database (Table 3). Three hours after the administration of CY, the major genes identified in C57BL/6J mouse cardiac tissue were those involved in dilated cardiomyopathy, hypertrophic cardiomyopathy, arrhythmogenic right ventricular cardiomyopathy, viral protein interactions with cytokines and their receptors, and extracellular matrix receptor interactions.

RT-PCR validation of microarray findings

Using RT-PCR and β-actin as a control, we examined the expression levels of 9 genes, including those important for myocardial function. The RT-PCR data confirmed the microarray analysis results (Fig. 3D). Figure 4 is a schematic diagram showing genes important for myocardial contraction in cardiomyocytes, with color-coded changes in expression.

Discussion

We examined ultrastructural alterations induced by high-dose CY administration in cardiac tissue using electron microscopic analysis. We found many structural changes in cardiomyocyte nuclear membranes, sarcoplasmic reticulum, mitochondria, and muscle fibers after high-dose CY administration. Changes in gene expression associated with high-dose CY administration were detected using comprehensive gene expression microarray analysis. In particular, most gene groups related to myocardial contraction and Ca^{2+} signaling pathways were suppressed. Changes observed in these gene groups were consistent with those observed in electron microscopy analysis. Genes that were altered by CY administration included oxidative stress-related genes, endoplasmic reticulum stress-related genes, apoptosis-related genes, *p53* expression-related genes, *p38MAPK*, GSK-3β, and Akt/PI3K signaling-related genes, among others. However, there have been no reports on the myocardial contraction or Ca^{2+} signaling pathway[19–24], which may represent a mechanism of CY myocardial damage that has not been previously identified.

The pumping action of the heart is performed by the contraction and relaxation of cardiomyocytes, which constitute the heart. These mechanisms are mainly controlled by the increase and decrease of intracellular Ca^{2+} concentration. The regulation of intracellular Ca^{2+} concentration is important for the heart to continuously and smoothly pump the blood throughout the body[25, 26]. The increase in intracellular Ca^{2+} concentration in the myocardium is triggered by a Ca^{2+} influx through L-type Ca^{2+} channels (DHPR) and Ca^{2+} release from the sarcoplasmic reticulum (RyR2) upon stimulation[27, 28]. The increased intracellular Ca^{2+} binds to troponin C (TnC), a subunit of the contractile regulatory protein troponin, and changes the steric configuration of tropomyosin, resulting in an interaction between actin and myosin. A contraction is induced by the interaction between actin and myosin. The decrease in intracellular Ca^{2+} concentration is caused by the uptake of sarco/endoplasmic reticulum Ca2+-ATPase

2A into the sarcoplasmic reticulum, extracellular efflux of the Na+/Ca^{2+} exchange system, or efflux by cell membrane Ca^{2+} pumps, which results in relaxation of the myocardium[29, 30]. In our experiments, gene expression levels of DHPR, RyR2, and TnC, which are important proteins involved in the regulation of Ca^{2+} concentration, were all decreased. Disruption of calcium regulatory mechanisms may cause elevated intracellular calcium concentrations, resulting in inflammation and apoptosis of cardiomyocytes, leading to myocardial contractile dysfunction. Based on the new mechanism identified in this study, CY myocardial injury may be prevented with a Ca^{2+} signaling sensitizer, such as levosimendan and pimobendan[31].

Concurrently, gene expression analysis after the administration of acrolein, which is considered to be the main driver of CY-related myocardial damage in in vitro research, revealed patterns that were different from those observed after the administration of CY. Acrolein is a small molecule that is highly reactive when exposed to unsaturated aldehyde and is quickly adsorbed by proteins and other substances[16, 17]. Therefore, it may be necessary to reexamine whether the acrolein dosage and method of administration in this study were appropriate. Furthermore, given the metabolism of CY, the myocardial injury model of CY may not be truly replicated unless acrolein is present in the myocardial cells. The present findings preclude any conclusions regarding the contribution of acrolein to CY cardiotoxicity.

N-acetylcysteine treatment significantly altered gene expression related to pathways such as chemical cardiogenesis-DNA adducts, complement and coagulation cascades, and retinol metabolism. NAC treatment significantly altered gene expression related to dilated cardiomyopathy, hypertrophic cardiomyopathy, and arrhythmogenic right ventricular cardiomyopathy. Electron microscopic findings were comparable to those of CY administration. Experimental methods used to evaluate NAC treatment require further research.

Conclusion

High-dose CY causes the expansion of transverse tubules and sarcoplasmic reticulum, the turbulence of myocardial fiber travel, and low density of contractile proteins in cardiomyocytes, as observed by electron microscopy. Microarray analysis revealed that high-dose CY treatment changed the cardiomyocyte expression of 1,210 genes associated with cardiomyopathy and cardiac muscle function. Gene expression profiles along with functional annotation clustering and the KEGG pathway functional classification analysis results suggest that CY-induced cardiotoxicity is associated with a disruption of the Ca^{2+} signaling pathway; these findings are consistent with the electron microscopy findings. The mechanism of CY cardiotoxicity identified in this study may help prevent adverse cardiac events in treatment.

Methods

Reagents

CY (CAS # 6055-19-2) and NAC (Sigma-Aldrich, St. Louis, MO) were dissolved in NS. Acrolein (10 mg/ml; AccuStandard®, New Heaven, CT) was dissolved in water.

Animals

Individual 5-week old female C57BL/6J mice (Charles River Japan, Kanagawa, Japan) were maintained at 22 ± 2 ℃ in 12-hour light/dark cycle (light from 7:00 to 19:00) and water and food *ad libitum*. Animals were sedated and anesthetized as follows agent. As the hypnotic sedative agent, 0.7 mg/kg of medetomidine hydrate, or analgesics agents, 4 mg/kg of midazolam and 5 mg/kg of butorphanol tartrate were mixed and dissolved in saline solution. All experiments were conducted in accordance with the ARRIVE guidelines and the Guideline for the Proper Conduct of Animal Experiments established by the Science Council of Japan, and were approved by the Institutional Animal Care and Use Committee of Kagoshima University, Kagoshima, Japan.

Plasma CY, HCY, and CEPM concentration after high-dose CY administration

To clarify the metabolic kinetics of CY, tail vein blood samples collected in EDTA2NA at 1 and 3 hours (or 4 hours for 400 mg/kg of CY) after a single intraperitoneal administration of CY (400 mg/kg to 700 mg/kg) were centrifuged at 2,000 rpm for 15 minutes, and plasma was collected (Supplemental Fig. 1). Concentrations of CY, HCY, and CEPM were determined by liquid chromatography/tandem mass spectrometry (LC/MS/MS), as previously described[9]. The area under the concentration-time curve (AUC) from zero to infinity was estimated using noncompartmental analysis based on the trapezoidal method in the MOMENT program, based on available data points.

Histological examinations

To examine pathological alteration associated with CY administration, mice were assigned randomly to a CY-treated group or a control group. For the control group, 250 µL of NS was administered intraperitoneally (i.p.) once a day for 2 days. Meanwhile, the CY-treated group received 250 µL of 400 mg/kg CY solution i.p. once a day for 2 days (Fig. 5A). In both groups, the animals were euthanized under anesthesia at 7 days after the last dose and hearts were collected. A section of the heart tissue was placed in 4% paraformaldehyde phosphate buffer solution (FUJIFILM Wako Chemicals, Tokyo, Japan) for HE staining. For electron microscopy analysis, another section of the heart was placed in 2.5% glutaraldehyde in 0.1 M phosphate buffer (pH 7.4), dehydrated in ethanol, and embedded in Epon 812 (TAAB Laboratories Equipment, Reading, UK). Ultrathin sections (80–90-nm) obtained, stained with uranyl acetate and lead citrate, and examined by electron microscopy (H-7600; Hitachi, Tokyo, Japan) at an acceleration voltage of 100 kV.

Detection of gene expression alterations

To elucidate the gene expression alteration induced by CY, animals were divided into four groups (Fig. 5B). NS was used as a negative control. CY-treated mice received 250 µL of 400 mg/kg CY solution

i.p. once a day for 2 days. The acrolein-treated group mice received 5 mg/kg of acrolein aqueous solution via i.p. Furthermore, to clarify the effect of NAC, 200 mg/kg of NAC solution was administered i.p. to NAC + CY group mice at 2 hours prior to CY administration (Fig. 5B). Three hours after the last dose, all animals were euthanized and hearts were harvested under anesthesia. A section of heart tissue was frozen in liquid nitrogen and stored at -80 ℃.

Total RNA isolation

Total RNA from the frozen heart tissue was isolated using NucleoSpin® RNA/Protein kit (MACHEREY-NAGEL., Düren, Germany), quantified using a SpectraMax ABS Plus (Molecular Devices, LLC. San Jose, CA), and assessed using an Experion automated electrophoresis station (Bio-Rad Laboratories Inc., Hercules, CA).

Gene expression microarrays

Microarray analysis was performed by Cell Innovator Inc. (Fukuoka, Japan). cDNA was amplified and labeled using Low Input Quick Amp Labeling (Agilent Technologies, Santa Clara, CA), hybridized using SurePrint G3 Mouse Gene Expression Microarray 8×60K v2 (Agilent), and scanned using an Agilent scanner. We used Agilent Feature Extraction Software (ver. 9.5.1.1; Agilent Technologies, Santa Clara, CA) to calculate relative hybridization intensities and background values.

Data analysis and filter criteria

We normalized raw signal intensities of samples (Control vs. CY, Control vs. Acrolein, and Control vs. NAC + CY) using the quantile algorithm in the preprocessCore library package[32] in the Bioconductor application[33], and selected probes with P flags in ≥ 1 sample. We used the normalized signal intensities of each probe to calculate intensity-based Z-scores[34] and ratios (non-log-scaled fold-change) to identify up- and down-regulated genes by comparison between control (no CY exposure) and experimental samples (CY, Acrolein, NAC + CY). Criteria were a Z-score of ≥ 2.0 and ratio of ≥ 1.5-fold for up-regulated genes, and a Z-score of ≤−2.0 and ratio of ≤ 0.66 for down-regulated genes. Significant over-representation of GO categories and significant pathway enrichment were determined using the Database for Annotation, Visualization, and Integrated Discovery (DAVID, 2021 update)[35], and functional annotation clustering and KEGG pathway functional classification analysis were performed[36]. We used MeV software[37] to generate a heat map and genes were sorted by the hierarchical clustering method, using color to indicate distance from the median of each row. Pearson correlation was used as the distance metric and, and average linkage clustering was the linkage method.

cDNA synthesis and RT-PCR

cDNA was synthesized from total RNA (see ‘total RNA isolation’ section) using PrimeScript™ RT (Takara Bio Inc., Otsu, Japan), and resulting cDNA was amplified using TB Green® Premix Ex Taq™ (Tli RNaseH Plus) (Takara Bio Inc., Otsu, Japan). RT-PCR was performed at 95°C for 30 sec, followed by 40 cycles alternating 95°C for 5 s and 60°C for 30 s using a Thermal Cycler Dice® Real Time System (Takara Bio Inc., Otsu, Japan). mRNA levels were calculated using cycle time (*Ct*) values normalized with actin beta

(Actβ) values. Using the $2^{-\Delta\Delta Ct}$ method[38], samples were compared using relative quantification (fold change) values.

Statistical analysis

R statistical software (version 3.4.2) was used for analyses. All data are means ± standard error. Between group differences were assessed by non-parametric Wilcoxon tests, and a p-value of less than 0.05 was considered significant. To detect significantly over-represented GO categories and to characterize functionally regulated gene groups, we used Fisher's exact test.

Declarations

Acknowledgements

Not applicable.

Author contributions

T.N. and E.M. directed the study, designed the study, and interpreted the results. E.M. performed experiments with mice. I.Y. conducted electron microscopy studies. H.H. conducted microarray analysis. K.I. conducted pharmacokinetics study and the analysis of CY data. E.M. summarized the results, performed image processing, and statistical analysis, and drafted the manuscript under the supervision of T.N.. S.N. Y.K. Y.K. and Y.O. coordinated the project and reviewed the manuscript. The final version of the manuscript was approved by all authors.

Data availability statement

Datasets and plugins for data processing used in this study are available from E.M. (k5424258@kadai.jp) upon reasonable request.

Competing interests

None

Additional information

Funding

Sponsors did not contribute to study design, data collection or analyses, or manuscript preparation.

T. Nishikawa received a Grant from Scientific Research (C) from the Ministry of Education, Culture, Sports, Science and Technology of Japan (Web: https://kaken.nii.ac.jp/ja/grant/KAKENHI-PROJECT-16K10034/; Grant Number, #16K10034).

E. Miyahara received a Grant from Grant-in-Aid for Early-Career Scientists from the Ministry of Education, Culture, Sports, Science and Technology of Japan (Web: https://kaken.nii.ac.jp/ja/grant/KAKENHI-PROJECT-21K15255/; Grant Number. #21K15255).

Ethics approval and consent to participate

The Ethics committee for Animal Experimentation at Kagoshima University (MD16074, MD18014, MD19088 and MD20052) approved this study.

References

1. Santos, G. W. *et al.* The use of cyclophosphamide for clinical marrow transplantation. *Transplant. Proc.* **4**, 559–564 (1972).
2. Emadi, A., Jones, R. J. & Brodsky, R. A. Cyclophosphamide and cancer: golden anniversary. Nat. Rev. Clin. Oncol. **6**, 638–647 (2009).
3. O'Donnell, P. V. *et al.* Nonmyeloablative bone marrow transplantation from partially HLA-mismatched related donors using posttransplantation cyclophosphamide. Biol. Blood Marrow Transplant. **8**, 377–386 (2002).
4. El Fakih, R. *et al.* Post-transplant cyclophosphamide use in matched HLA donors: a review of literature and future application. Bone Marrow Transplant. **55**, 40–47 (2020).
5. Atalay, F., Gulmez, O. & Ozsancak Ugurlu, A. Cardiotoxicity following cyclophosphamide therapy: a case report. J. Med. Case Rep. **8**, 252 (2014).
6. Dhesi, S. *et al.* Cyclophosphamide-induced cardiomyopathy: a case report, Review, and Recommendations for Management. J. Investig. Med. High Impact Case Rep. **1**, 2324709613480346 (2013).
7. Gottdiener, J. S., Appelbaum, F. R., Ferrans, V. J., Deisseroth, A. & Ziegler, J. Cardiotoxicity associated with high-dose cyclophosphamide therapy. Arch. Intern. Med. **141**, 758–763 (1981).
8. McDonald, G. B. *et al.* Cyclophosphamide metabolism, liver toxicity, and mortality following hematopoietic stem cell transplantation. Blood **101**, 2043–2048 (2003).
9. Nishikawa, T. *et al.* Mechanisms of fatal cardiotoxicity following high-dose cyclophosphamide therapy and a method for its prevention. PLOS ONE **10**, e0131394 (2015).
10. Kurauchi, K., Nishikawa, T., Miyahara, E., Okamoto, Y. & Kawano, Y. Role of metabolites of cyclophosphamide in cardiotoxicity. BMC Res. Notes **10**, 406 (2017).
11. Yoshida, M. *et al.* Acrolein toxicity: comparison with reactive oxygen species. Biochem. Biophys. Res. Commun. **378**, 313–318 (2009).
12. Lau, S. *et al.* Effects of acrolein in comparison to its prodrug cyclophosphamide on human primary endothelial cells in vitro. Toxicol. In Vitro **62**, 104685 (2020). 10.1016/j.tiv.2019.104685.
13. Dionísio, F. *et al.* Cardiotoxicity of cyclophosphamide's metabolites: an in vitro metabolomics approach in AC16 human cardiomyocytes. Arch. Toxicol. **96**, 653–671 (2022).

14. Podgurskaya, A. D. *et al.* Cyclophosphamide arrhythmogenicitytesting using human-induced pluripotent stem cell-derived cardiomyocytes. Sci. Rep. **11**, 2336 (2021).
15. Liu, W. *et al.* Aldehyde dehydrogenase 2 activation ameliorates cyclophosphamide-induced acute cardiotoxicity via detoxification of toxic aldehydes and suppression of cardiac cell death. J. Mol. Cell. Cardiol. **121**, 134–144 (2018).
16. Muguruma, K. *et al.* Disease-associated acrolein: A possible diagnostic and therapeutic substrate for in vivo synthetic chemistry. Bioorg. Med. Chem. **28**, 115831 (2020).
17. Kehrer, J. P. & Biswal, S. S. The molecular effects of acrolein. Toxicol. Sci. **57**, 6–15 (2000).
18. Edgar, R., Domrachev, M. & Lash, A. E. Gene expression omnibus: NCBI gene expression and hybridization array data repository. Nucleic Acids Res. **30**, 207–210 (2002).
19. Iqubal, A. *et al.* Molecular mechanism involved in cyclophosphamide-induced cardiotoxicity: old drug with a new vision. Life Sci. **218**, 112–131 (2019).
20. Song, Y. *et al.* Ferulic acid against cyclophosphamide-induced heart toxicity in mice by inhibiting NF-κB pathway. *Evid. Based Complement. Alternat. Med.* 2016, 1261270 (2016).
21. Fatani, A. G. *et al.* Carnitine deficiency aggravates cyclophosphamide-induced cardiotoxicity in rats. Chemotherapy **56**, 71–81 (2010).
22. Asiri, Y. A. Probucol attenuates cyclophosphamide-induced oxidative apoptosis, p53 and Bax signal expression in rat cardiac tissues. Oxid. Med. Cell. Longev. **3**, 308–316 (2010).
23. Park, E. S. *et al.* Cardioprotective effects of rhamnetin in H9c2 cardiomyoblast cells under H_2O_2-induced apoptosis. J. Ethnopharmacol. **153**, 552–560 (2014).
24. El-Agamy, D. S., Elkablawy, M. A. & Abo-Haded, H. M. Modulation of cyclophosphamide- induced cardiotoxicity by methyl palmitate. Cancer Chemother. Pharmacol. **79**, 399–409 (2017).
25. Bers, D. M. *Excitation-Contraction Coupling and Cardiac Contractile Force* (Springer, Dordrecht, Netherlands, 2001); ISBN 978-0-7923-7158-8.
26. Avila, G., de la Rosa, J. A., Monsalvo-Villegas, A. & Montiel-Jaen, M. G. Ca^{2+} channels mediate bidirectional signaling between sarcolemma and sarcoplasmic reticulum in muscle cells. Cells **9**, 9(1):55 (2019).
27. Protasi, F. Structural interaction between RYRs and DHPRs in calcium release units of cardiac and skeletal muscle cells. Front. Biosci. **7**, d650–d658 (2002).
28. Ríos, E., Figueroa, L., Manno, C., Kraeva, N. & Riazi, S. The couplonopathies: A comparative approach to a class of diseases of skeletal and cardiac muscle. J. Gen. Physiol. **145**, 459–474 (2015,).
29. Rossi, A. E. & Dirksen, R. T. Sarcoplasmic reticulum: the dynamic calcium governor of muscle. Muscle Nerve **33**, 715–731 (2006).
30. Tadini-Buoninsegni, F., Smeazzetto, S., Gualdani, R. & Moncelli, M. R. Drug interactions with the Ca^{2+}-ATPase from sarco (Endo) plasmic reticulum (SERCA). Front. Mol. Biosci. **5**, 36 (2018).
31. Endoh, M. Cardiac Ca^{2+} signaling and Ca^{2+} sensitizers. Circ. J. **72**, 1915–1925 (2008).

32. Bolstad, B. M., Irizarry, R. A., Astrand, M. & Speed, T. P. A comparison of normalization methods for high density oligonucleotide array data based on variance and bias. Bioinformatics **19**, 185–193 (2003).
33. Robert, C. Gentleman. *et al*. Bioconductor: open software development for computational biology and bioinformatics. Genome Biol. **5**, R80 (2004).
34. Quackenbush, J. Microarray data normalization and transformation. *Nat. Genet.* **32** Supplement, 496–501 (2002).
35. Huang, D. W., Sherman, B. T. & Lempicki, R. A. Systematic and integrative analysis of large gene lists using DAVID bioinformatics resources. Nature Protoc. **4**, 44–57 (2009).
36. Kanehisa, M. & Goto, S. KEGG: kyoto encyclopedia of genes and genomes. Nucleic Acids Res. **28**, 27–30 (2000).
37. Saeed, A. I. *et al.* TM4: a free, open-source system for microarray data management and analysis. BioTechniques **34**, 374–378 (2003).
38. Livak, K. J. & Schmittgen, T. D. Analysis of relative gene expression data using real-time quantitative PCR and the 2(-Delta Delta C (T)) method. Methods. **25**, 402–408 (2001).

Tables

Tables 1 to 3 are available in the Supplementary Files section.

Figures

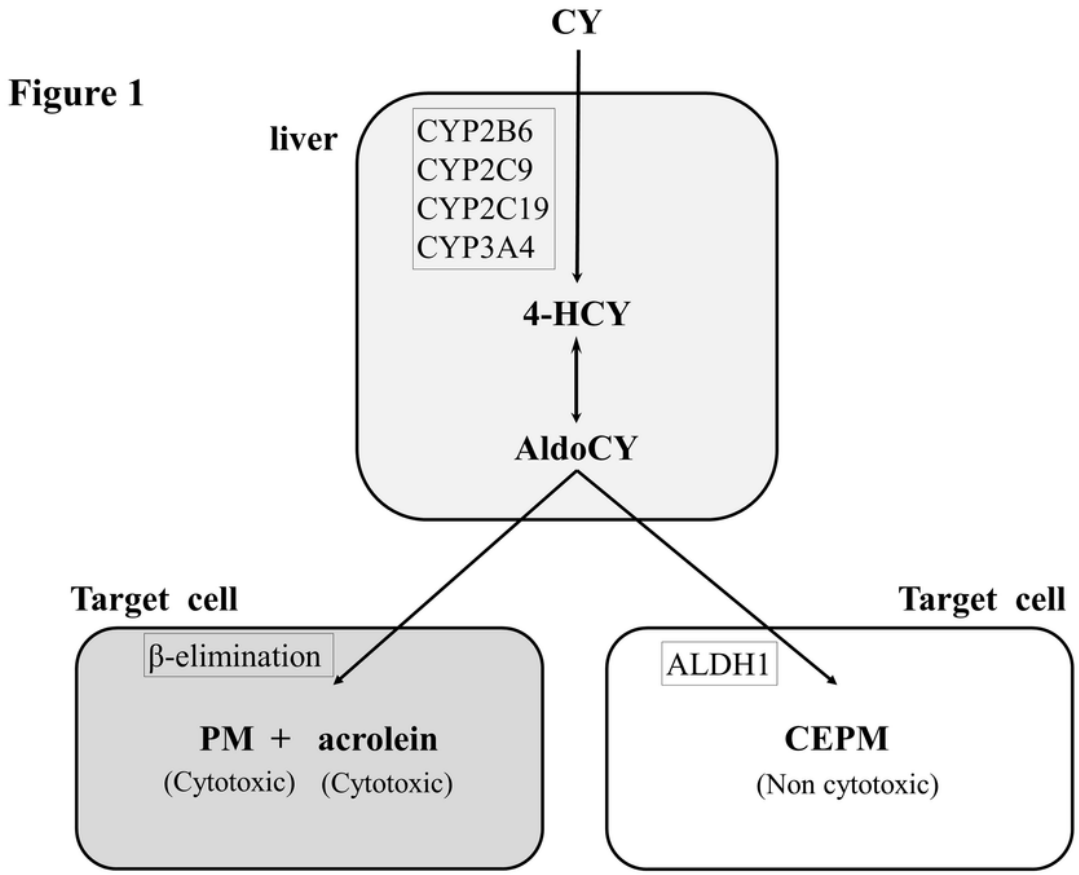

Figure 1

Metabolic pathway of cyclophosphamide. The hepatic cytochrome P-450 enzyme (CYP) system (CYP2B6, 2C9, 2C19, and 3A4) metabolizes cyclophosphamide (CY) to 4-hydroxy-cyclophosphamide (4-HCY). Subsequently, 4-HCY is oxidized to its tautomer aldocyclophosphamide (AldoCY), absorbed by cells, and converted to phosphoramide mustard (PM) and acrolein by β-elimination. AldoCY can be oxidized to o-carboxyethylphosphoramide mustard (CEPM) by aldehyde dehydrogenase 1 (ALDH1).

Figure 2

Figure 2

Figure 2

Effect of cyclophosphamide (CY) on mouse cardiac tissue. Light microscope examination of mice left ventricle cardiac tissue stained with hematoxylin and eosin was performed for mice treated with saline (A and B, 100x magnification) and for mice treated with CY (C and D, 400x magnification). B and D images are magnified versions of A and C images, respectively. Panels E-J show images of the ultra-structure of mice cardiac tissue treated CY. The squares in panel E show extension of transverse tubules and sarcoplasmic reticulum. Arrows defined by outlines in panels E and F show lamellar bodies. The circled areas in F show mitochondria that have either lost or expanded their internal structure. Black arrows in panel F show lipid droplets. Panels G and F show the turbulence of myocardial fiber travel. The dark area surrounded by a square shows muscle contractile fiber structures with different contractile states from within the same muscle cell. Panel J shows low-density contractile proteins in a cardiomyocyte.

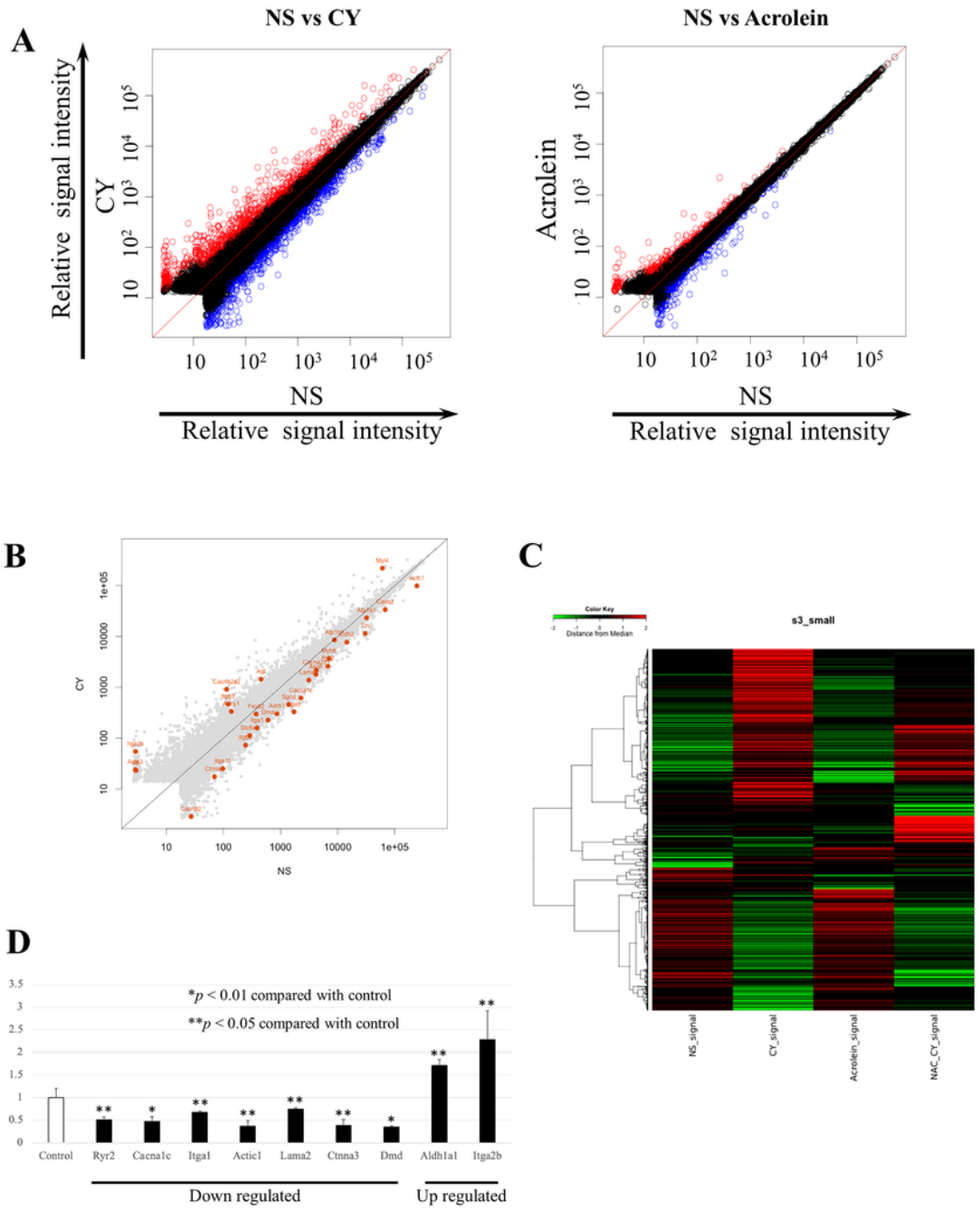

Figure 3

Gene expression profiles. (A) Scatterplots of the gene expression in C57BL/6J mice administered cyclophosphamide (CY) or acrolein. The X-axis is relative normalized log_2-signal intensity of control (NS) samples, and the Y-axis is normalized log_2-signal intensity of CY or acrolein samples. (A) Blue dots and red dots indicate down-regulated and up-regulated genes, respectively. (B) Scatterplots highlighting genes associated with myocardial contraction. (C) Clustering diagram of gene trees and heatmap generated by

MeV software using the hierarchical clustering (HCL) method to sort the genes, with Pearson correlation estimates as distance metrics and average linkage clustering as the linkage method. Red and green blocks represent high and low levels of expression, respectively, relative to control; black blocks indicate expression levels similar to control. (D) Gene expression levels, as detected by RT-PCR, associated with myocardial contraction after CY administration.

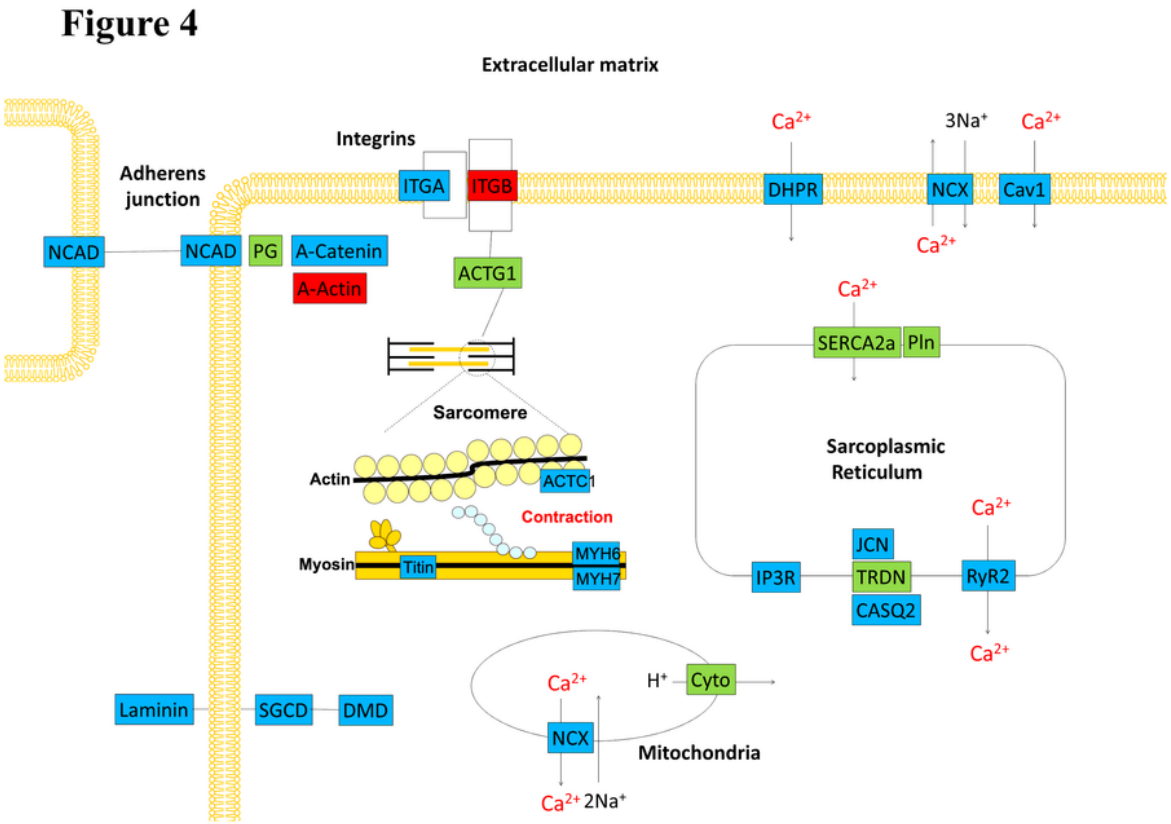

Figure 4

Schematic drawing of gene expression profile in cardiac tissue of a C57BL/6J mouse. Red boxes denote up-regulated genes 3 hours after treatment with cyclophosphamide. Blue boxes denote down-regulated genes. Green bozes show genes whose expression did not change.

Figure 5

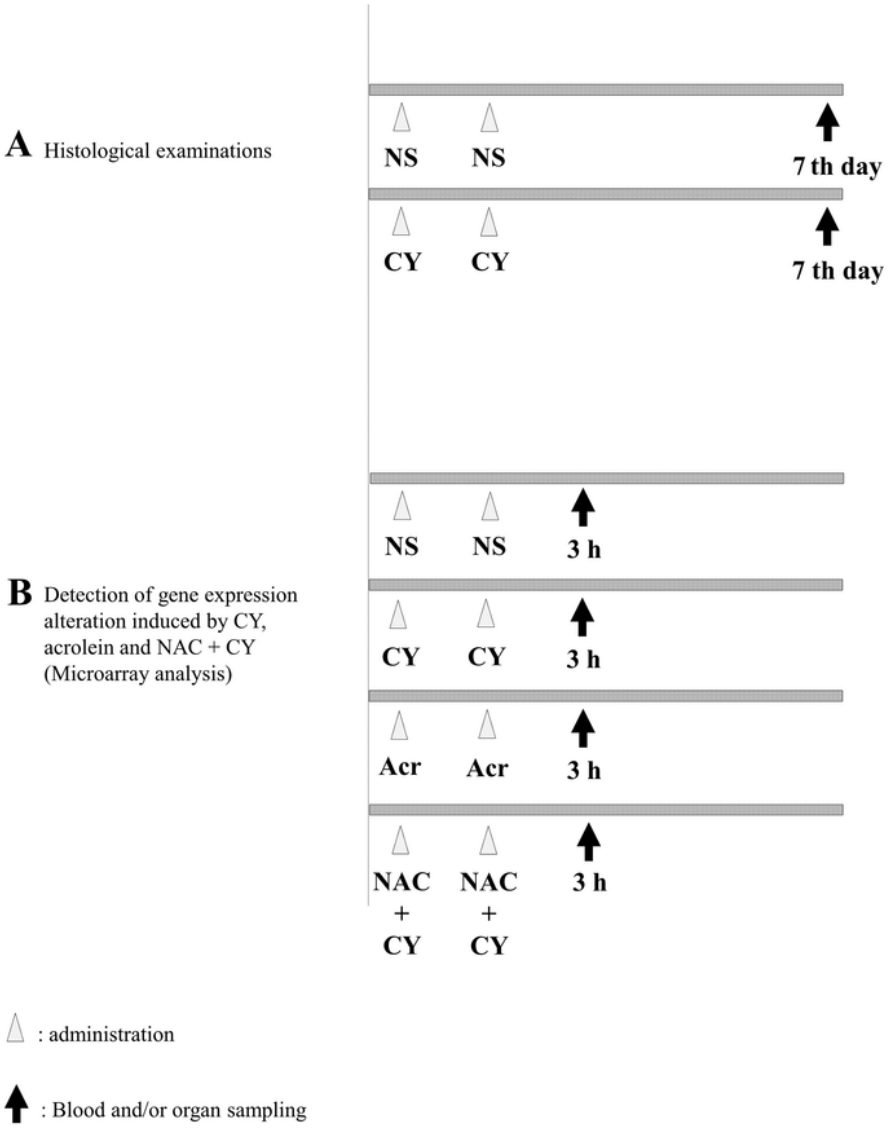

Figure 5

Experimental procedures. (A) C57BL/6J mice (females aged 6 weeks) were treated intraperitoneally with normal saline (control) or 400 mg/kg of cyclophosphamide (CY) once daily for 2 consecutive days. Seven days after the last dose, mice were euthanized under anesthesia and hearts were collected. (B) C57BL/6J mice (females aged 6 weeks) were treated intraperitoneally with normal saline (control), 400 mg/kg of CY, 5 mg/kg of acrolein, or 400 mg/kg of CY with 200 mg/kg of N-acetylcysteine (NAC) once daily for 2 consecutive days. NAC was used 2 hours before CY administration. Three hours after the last dose, mice were euthanized under anesthesia and hearts were collected.

Supplementary Files

This is a list of supplementary files associated with this preprint. Click to download.

- HDCYmicroarraytable.docx
- Supplementaryinformation.docx